Heliyon 10 (2024) e25248

Contents lists available at ScienceDirect

Heliyon

journal homepage: www.cell.com/heliyon

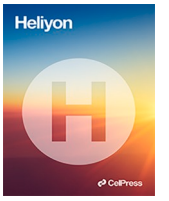

Research article

Stereoselective synthesis and X-ray structure determination of novel 1,2-dihydroquinolinehydrazonopropanoate derivatives

Hendawy N. Tawfeek [a,*], Ahmed M. Tawfeek [b], Stefan Bräse [c,**], Martin Nieger [d], Essmat M. El-Sherief [a]

[a] Chemistry Department, Faculty of Science, Minia University, El-Minia, 61519, Egypt
[b] Chemistry Department, College of Science, King Saud University, Riyadh, 11451, Saudi Arabia
[c] Institute of Biological and Chemical Systems, IBCS-FMS, Karlsruhe Institute of Technology, 76131, Karlsruhe, Germany
[d] Department of Chemistry, University of Helsinki, PO Box 55, A. I. Virtasen Aukio 1, 00014, Helsinki, Finland

ARTICLE INFO

Keywords:
Aza-michael addition
Hydrazono-hydrazides
Stereoselective synthesis
4-Hydrazinyl-quinolin-2(1*H*)-Ones
Ethyl propiolate
1,2-Dihydroquinolin-4-yl(hydrazono) propanoate and X-ray crystallography

ABSTRACT

A novel series of 1,2-dihydroquinolinhydrazonopropanoate have been synthesized *via* a convenient aza-Michael addition reaction between hydrazinylquinolinones and ethyl propiolate in ethanol under refluxing temperature. The structures for all obtained products were confirmed with FTIR, NMR spectrums, as well as mass spectrometry. In addition, the monoclinic structure for compounds **8a**, **8c,** and **8d** was also confirmed *via* X-ray crystallography analyses. The *E*-configuration for the obtained products was confirmed form the X-ray analysis. On the other hand, the crystal packing shows that the intermolecular and hydrogen bonds between atoms are parallel to the bc plan.

1. Introduction

As privileged structural subunits, quinolones have been witnessed in many biologically active compounds and natural products [1–3]. Moreover, 4-hydroxyquinolone, as well as *Skimmianine*, proven as an effective anti-cancer agent [4], and *Flindersine*, playing an antibacterial and antifungal activity [5], were examples of naturally extracting quinolone derivatives (Fig. 1). Quinoline derivatives possess peptide bonds like Pipestelide C that was isolated from a marine fungus **(**Fig. 1**)** [6].

On the other hand, there were synthetic drugs based on the main quinolinone unit on their structures, such as L-701,324, which represented a selective antagonist at the glycine site of the NMDA receptor and counteracts haloperidol-induced muscle rigidity in rats [7], the other was benzothiadiazinyl quinolinedione described to be an inhibitor of the RNA-dependent RNA polymerase enzyme transcribed by the Hepatitis C virus (Fig. 2) [8].

Douche et al. have reported the synthesis of imidazolylquinoline derivatives, which have been investigated as potential antiviral SARS-CoV-2 candidate [9].

The hydrazide-hydrazone moiety –NHN═CH has been an important structure group for various biological activities, including antibacterial, antifungal, analgesic, anti-inflammatory, antidepressant, and anti-cancer activities [10–12]. Using the hydrazide-hydrazone moiety in conjunction with a quinoline system, supporting their activities as antimicrobial [13],

* Corresponding author. Chemistry Department, Faculty of Science, Minia University, El-Minia, 61519, Egypt.
** Corresponding author. Institute of Biological and Chemical Systems, IBCS-FMS, Karlsruhe Institute of Technology, 76131 Karlsruhe, Germany.
E-mail addresses: hendawy1976@yahoo.com (H.N. Tawfeek), braese@kit.edu (S. Bräse).

https://doi.org/10.1016/j.heliyon.2024.e25248
Received 29 September 2023; Received in revised form 22 January 2024; Accepted 23 January 2024
Available online 1 February 2024

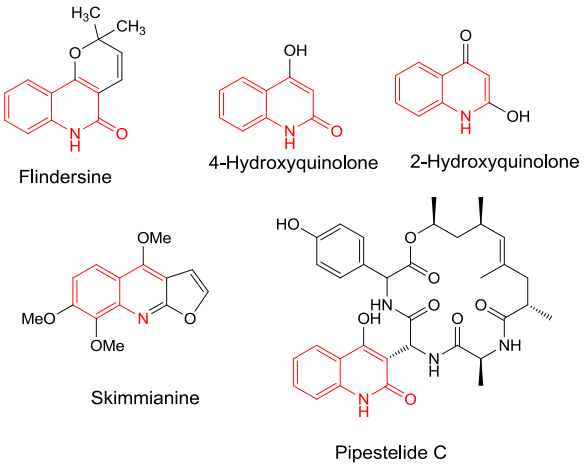

Fig. 1. Naturally occurring quinolone-related structures.

Fig. 2. Vital drugs, including quinolinone ring.

antimycobacterial [14], anti-tubercular [15,16], anticonvulsant [17], and cytotoxic activity [18,19]. These biological activities are attributed to the numerous interesting and important properties of the hydrazide-hydrazone moiety, for example, their relatively higher metabolic stability towards proteases than amides and their tunable, labile nature in acidic pH [20].

Thus, the developing efficient strategies for constructing such frameworks has attracted the growing interest of synthetic chemists. The last decade has shown significant progress in quinolone derivatives synthesis and biological evaluation, owing to their wide application in medicinal chemistry.

Elbastawesy et al. have reported the synthesis of 6-substituted quinoline-2-one thiosemicarbazides, and their activities were evaluated *invitro* against the urease-producing *R. mucilaginosa* and *Proteus mirabilis* bacteria as fungal and bacterial [21].

Valencia et al. have reported the synthesis of quinolone-based thiosemicarbazones and investigated their *invitro* activities against *Mycobacterium tuberculosis* (*M. tuberculosis*) [22]. However, the reaction of hydrazinyl quinolone with tetracyanoethylene (TCNE) was carried out by Elbastawesy et al. to afford pyrazolyl quinolone derivatives and their biological activities as potential apoptotic anti-proliferative agents targeting the EGFR inhibitory pathway have been investigated [23].

Recently, Al-Wahaibi et al. have constructed azaspiroquinolone derivatives *via* a one-pot reaction between hydrazinylquinolones, cyclic ketones, and thioglycolic acid, alongside studying the biological properties of the synthesized compounds as antiproliferative against four cancer cells [24].

Here, we have reported the reaction of hydrazonylquinolones as donating molecules with a π-deficient molecule ethyl propynolate, which possess a C≡C bond attached to an electron-withdrawing group. Our expected goal is to synthesize a pyrazoloquinolinone ring *via* nucleophilic attack of the hydrazinyl moiety into the triple bond followed by cyclization. Unfortunately, the analyses and the X-ray measurements clarified that 1,2-dihydroquinolinehydrazonopropanoate derivatives were formed without internal cyclization occurring. The reaction proceedes *via* nucleophilic addition of a nucleophile ($QNHNH_2$, donor) on the alkyne ($HC{\equiv}CCOOCH_2CH_3$, Michael acceptor) in agree with aza-Michael addition reaction [25,26].

2. Experiments

Melting points were measured by a Stuart melting point apparatus and were uncorrected. The IR spectra were recorded using an FTIR Alpha 24 spectrophotometer as KBr pellets. The ^1H and ^{13}C NMR spectra were recorded in DMSO–*d*6 as a solvent on Varian Gemini NMR spectrometer at 400 and 100 MHz, respectively, using TMS as an internal standard. Chemical shifts were reported as δ values (ppm), while couplings constants (*J*) are measured in hertz (Hz). Some NMR spectra were measured in DMSO-d_6 on a Bruker spectrometer (300 MHz for ^1H and 75 MHz for ^{13}C) at MICROANALYICAL CENTER, Cairo University. Mass spectra were recorded by a MAT 95 +FAB mass spectrometer in EI (70 eV) model. The reactions were closely monitored with TLC (thin-layer chromatography) on

Merck alumina-backed TLC plates Pf_{254} using UV light.

2.1. Chemistry

The starting materials were prepared according to the reported articles [27–29], with slight modification in the preparation of hydrazinylquinolones **5a-g** 4-chloroquinolones **4a-g** and were refluxed with hydrazine hydrate for 3 h. Hydrzine hydrate acted as reagent and solvent. The formed precipitate was filtered, flushed several times with water, and used for the second step without further purifications.

2.2. Synthesis of quinolone hydrazonopropanoates

In a round bottomed flask (50 ml), substituted hydrazinyl quinolone-2-one (1 mmol) suspended in ethanol (10 ml) ethyl propiolate (1.2 mmol) was added, the mixture was refluxed for about 6 h. The reaction was monitored with TLC, until the starting spot disappeared. The formed precipitate was filtered off, flushed several times with hot ethanol, dried, and recrystallized using methanol furnished 1,2-dihydroquinolin ehydrazono propanoate derivatives **8a-g**. Single crystals, suitable for X-ray crystallographic analyses for compounds **8b**, **8c,** and **8d**, have been obtained using methanol as the choice solvent of crystallization.

2.3. (E)-Ethyl 3-(2-(1-methyl-2-oxo-1,2-dihydroquinolin-4-yl)hydrazono)propanoate (8a)

Pale yellow crystals (methanol), (258 mg, 90 %), Mp 190 °C; IR (KBr): ν 3237 (NH), 3085 (aryl-CH), 2991 (str., ali-CH), 1736 (ester-CO) 1628 (amide-CO), 1602 (C═N), 1554 (C═C) cm^{-1}. ^{1}H NMR (300 MHz, DMSO-d_6): $\delta_H = 1.22$ (t, $J = 6.9$ Hz; 3H, CH_3); 3.44 (s, 3H, N–CH_3); 3.51–3.53 (d, $J = 11.4$ Hz; 2H, –CH_2-CH═N) [25,30]; 4.12–4.14 (q, $J = 6.9$ Hz; 2H, CH_2O); 6.17 (s, 1H, H-3); 7.22–7.28 (m, 1H, quinolinone-H); 7.43–7.48 (m, 1H, quinolinone-H); 7.60–7.64 (m, 1H, quinolinone-H); 7.73–78 (m, 1H, quinolinone-H); 8.06 (t, $J = 11.4$ Hz; 1H, CH═N); 10.55 (brs, 1H, hydrazono-NH) ppm. ^{13}C NMR (75 MHz, DMSO-d_6): $\delta_C = 14.14$ (CH_3-ethyl); 28.50 (N–CH_3); 37.88 (*C*H_2–CH═N); 60.49 (-CH_2O); 93.63 (C-3); 112.82 (C-4a); 115.16 (C-8); 120.96 (C-6); 122.35 (C-5); 131.09 (C-7); 140.05 (C-8a); 141.35 (C-4); 147.44 (CH═N-); 162.03 (C-2); 169.83 (ester-CO) ppm. MS (EI, 70 eV): *m/z* (%) 288 [M^+, 100].

2.4. (E)-Ethyl 3-(2-(2-oxo-1,2-dihydroquinolin-4-yl)hydrazono)propanoate (8b)

Pale yellow crystals (methanol), (278 mg, 92 %), Mp 245 °C; ^{1}H NMR (400 MHz, DMSO-d_6): $\delta_H = 1.26$ (t, $J = 8.0$ Hz, 3H, CH_3); 3.48–3.51 (d, $J = 16.0$ Hz, 2H, –CH_2-CH═N) [30]; 4.16 (q, $J = 8.0$ Hz; 2H, CH_2O); 6.08 (s, 1H, quinolinone-H-3); 7.10–7.18 (m, 1H, quinolinone-H); 7.26–7.31 (m, 1H, quinolinone-H); 7.45–7.55 (m, 1H, quinolinone-H); 7.78 (s, 1H, quinolinone-H); 8.08 (t, $J = 16.0$ Hz, 1H, CH═N); 10.50 (brs, 1H, hydrazono-NH); 11.00 (brs, 1H, q quinolinone-NH) ppm. ^{13}C NMR (100 MHz, DMSO-d_6): $\delta_C = 14.05$ (CH_3-ethyl); 37.76 (*C*H_2–CH═N); 60.49 (-CH_2O); 93.49 (C-3); 111.71 (C-4a); 115.93 (C-8); 120.61 (C-6); 121.87 (C-5); 130.35 (C-7); 139.32 (C-8a); 141.13 (C-4); 148.45 (CH═N-); 162.79 (C-2); 169.72 (ester-CO) ppm.

2.5. (E)-Ethyl 3-(2-(6-methoxy-2-oxo-1,2-dihydroquinolin-4-yl)hydrazono)propanoate (8c)

Pale yellow crystals (methanol), (278 mg, 92 %), Mp 245 °C; IR (KBr): ν 3163 (NH), 3055 (aryl-CH), 2996 (str., ali-CH), 1727 (ester-CO) 1638 (amide-CO), 1604 (C═N), 1546 (C═C) cm^{-1}. ^{1}H NMR (400 MHz, DMSO-d_6): $\delta_H = 1.26$ (t, J = 8.0, 3H, CH_3); 3.44 (d, J = 16.0, 2H, –CH_2-CH =); 3.80 (s, 3H, CH_3O); 4.14 (q, $J = 8.0$ Hz; 2H, CH_2O); 6.06 (s, H-3); 7.20 (m, 2H, quinolinone-H); 7.52 (s, 1H, quinolinone-H); 7.74 (t, $J = 16.0$ Hz, 1H, CH═N) [30]; 10.45 (brs, 1H, hydrazono-NH); 10.95 (brs, 1H, quinolinone-NH) ppm. ^{13}C NMR (100 MHz, DMSO-d_6): $\delta_C = 14.05$ (CH_3-ethyl); 37.74 (*C*H_2–CH═N); 55.59 (CH_3O); 60.51 (-CH_2O); 93.05 (C-3); 112.01 (C-4a); 117.74 (C-8); 119.54 (C-5); 133.55 (C-7); 140.93 (C-8a); 143.31 (C-6); 148.9 (CH═N); 153.63 (C-4); 162.39 (C-2); 169.76 (ester-CO) ppm. MS (EI, 70 eV): *m/z* (%) 303 [M^+, 100].

2.6. (E)-Ethyl 3-(2-(6-methyl-2-oxo-1,2-dihydroquinolin-4-yl)hydrazono)propanoate (8d)

Pale yellow crystals (methanol), (278 mg, 92 %), Mp 245 °C; ^{1}H NMR (400 MHz, DMSO-d_6): $\delta_H = 1.28$ (t, $J = 8.0$ Hz, 3H, CH_3); 3.44 (d, $J = 12.0$ Hz, 2H, –CH_2-CH═N); 4.09–4.18 (q, $J = 8.0$ Hz; 2H, CH_2O); 6.07 (s, 1H, quinolinone-H-3); 7.13–7.20 (m, 1H, quinolinone-H); 7.28–7.33 (m, 1H, quinolinone-H); 7.73–7.82 (m, 2H, quinolinone-H and CH═N); 10.51 (brs, 1H, hydrazono-NH); 10.98 (brs, 1H, quinolinone-NH) ppm. ^{13}C NMR (100 MHz, DMSO-d_6): $\delta_C = 14.03$ (CH_3-ethyl); 20.58 (CH_3); 37.76 (*C*H_2–CH═N); 60.66 (CH_2O); 93.60 (C-3); 111.61 (C-4a); 115.70 (C-8); 127.32 (C-5); 129.66 (C-7); 137.26 (C-6); 140.99 (C-8a); 148.32 (CH═N); 162.78 (C2); 169.12 (ester-CO) ppm. *Anal. Calcd for* $C_{15}H_{17}N_3O_3$: C, 62.71; H, 5.96; N, 14.63. Found: C, 62.66; H, 5.88; N, 14.52.

2.7. Ethyl (E)-3-(2-(6-chloro-2-oxo-1,2-dihydroquinolin-4-yl)hydrazineylidene)propanoate (8e)

Pale yellow crystals (methanol), (267 mg, 87 %), Mp 181 °C; IR (KBr): ν 3232, 3152 (NH's), 3070 (aryl-CH), 2985 (str., ali-CH), 1734 (ester-CO) 1641 (amide-CO), 1595 (C═N), 1544 (C═C) cm^{-1}. ^{1}H NMR (300 MHz, DMSO-d_6): $\delta_H = 1.23$ (t, $J = 7.2$ Hz; 3H, CH_3); 3.42–3.3.44 (d, $J = 11.4$ Hz; 2H, –CH_2-CH═N); 4.15 (q, $J = 7.2$ Hz; 2H, CH_2O); 6.06 (s, 1H, H-3); 7.26–7.30 (m, 1H, quinolinone-H); 7.48–7.51 (m, 1H, quinolinone-H); 7.71–7.75 (t, $J = 11.4$ Hz; 1H, CH═N); 10.56 (brs, 1H, hydrazono-NH); 11.20 (brs, 1H,

quinolinone-NH) ppm. ^{13}C NMR (75 MHz, DMSO-d_6): δ_C δ_C = 14.10 (CH_3-ethyl); 37.83 (CH_2–CH═N); 60.61 (CH_2O); 94.33 (C-3); 112.92 (C-4a); 117.58 (C-8); 121.46 (C-5); 125.15 (C-7); 130.37 (C-6); 138.14 (C-8a); 141.78 (C-4); 147.79 (CH═N); 162.80 (C2); 169.72 (ester-CO) ppm. MS (EI, 70 eV): *m/z* (%) 307 [M^+, 100].

2.8. Ethyl (E)-3-(2-(7-methyl-2-oxo-1,2-dihydroquinolin-4-yl)hydrazineylidene)propanoate (8f)

Pale yellow crystals (methanol), (245 mg, 85 %), Mp 207 °C; IR (KBr): ν 3243, 3159 (NH's), 3067 (aryl-CH), 2936 (str., ali-CH), 1733 (ester-CO) 1630 (amide-CO), 1598 (C═N), 1526 (C═C) cm^{-1}. ^{1}H NMR (300 MHz, DMSO-d_6): δ_H = 1.26 (t, J = 7.2 Hz; 3H, CH_3-ethyl); 2.82 (s, 3H, CH_3); 3.42 (d, J = 11.4 Hz, 2H, –CH_2-CH═N); 4.16 (q, J = 7.2 Hz; 2H, CH_2O); 6.18 (s, 1H, H-3); 698 (m, 1H, quinolinone-H); 7.31 (m, 1H, quinolinone-H); 7.63 (t, J = 11.4 Hz; 1H, CH═N); 7.84–7.87 (m, 2H, quinolinone-H); 10.48 (brs, 1H, hydrazono-NH); 11.18 (brs, 1H, quinolinone-NH) ppm. ^{13}C NMR (75 MHz, DMSO-d_6): δ_C = 14.12 (CH_3-ethyl); 21.18 (CH_3); 37.86 (CH_2–CH═N); 60.81 (CH_2O); 92.88 (C-3); 112.19 (C-4a); 115.61 (C-8); 125.11 (C-6); 129.78 (C-5); 134.65 (C-7); 138.51 (C-8a); 141.83 (C-4); 148.62 (CH═N); 162.30 (C2); 168.72 (ester-CO) ppm. MS (EI, 70 eV): *m/z* (%) 287 [M^+, 100].

2.9. Ethyl (E)-3-(2-(8-methyl-2-oxo-1,2-dihydroquinolin-4-yl)hydrazineylidene)propanoate (8g)

Pale yellow crystals (methanol), (251 mg, 82 %), Mp 224 °C; IR (KBr): ν 3236, 3163 (NH's), 3076 (aryl-CH), 2996 (str., ali-CH), 1737 (ester-CO) 1625 (amide-CO), 1606 (C═N), 1546 (C═C) cm^{-1}. ^{1}H NMR (300 MHz, DMSO-d_6): 1.24 (t, J = 7.2 Hz; 3H, CH_3-ethyl); 3.44 (d, J = 12.0 Hz; 2H, –CH_2-CH═N) [30]; 2.39 (s, 3H, CH_3); 4.16 (q, J = 7.2 Hz; 2H, CH_2O); 6.06 (s, 1H, H-3); 7.09 (m, 1H, quinolinone-H); 7.35 (m, 1H, Ar–H); 7.76 (t, 12.0 Hz; 1H, CH═N); 7.85 (m, 2H, quinolinone-H); 10.08 (brs, 1H, hydrazono-NH); 10.49 (brs, 1H, quinolinone-NH) ppm. ^{13}C NMR (75 MHz, DMSO-d_6): δ_C = 14.09 (CH_3-ethyl); 17.63 (CH_3); 37.83 (CH_2–CH═N); 60.55 (CH_2O); 93.51 (C-3); 111.64 (C-4a); 119.77 (C-5); 120.47 (C-6); 123.80 (C-8); 131.69 (C-7); 137.64 (C-8a); 141.27 (C-4); 148.95 (CH═N); 163.09 (C2); 169.77 (ester-CO) ppm. MS (EI, 70 eV): *m/z* (%) 307 (M^++H_2O, 35); 289 (M^+, 15), 190 (3).

2.10. Single crystal X-ray structure determination of 8b, 8c, and 8d

Single crystals generated by slow evaporation from methanol. A good crystal with a suitable size was selected for X-ray diffraction analysis.

The single-crystal X-ray diffraction study was carried out on a Bruker D8 Venture diffractometer with a PhotonII detector at 173(2) K or 298(2) K using Cu-Kα radiation (λ = 1.54178 Å). Dual space methods (SHELXT) [31] were employed for the structure solution, and refinement was carried out using SHELXL-2014 (full-matrix least-squares on F^2) [32]. Hydrogen atoms were refined using a riding model (H(O) free, except MeOH in **8b**). Semi-empirical absorption corrections were applied; for **8b,** an extinction correction was applied.

2.11. Compound **8b**

$C_{14}H_{15}N_3O_3{\cdot}0.5(CH_4O){\cdot}0.5(H_2O)$, Mr = 298.32 g mol^{-1}, blocks yellow, size = 0.12 × 0.06 × 0.04 mm, monoclinic, *C2/c* (no.15), a = 16.981 (6) Å, b = 11.048 (4) Å, c = 16.479 (5) Å, β = *98.60 (2)*°, λ = 1.54178 Å, V = 3056.8 (18) Å^3, Z = 8, D_{calcd} = 1.296 Mg m^{-3}, F (000) = 1264, μ = 0.80 mm^{-1}, T = 298 K, 13838 measured reflections ($2\theta_{max}$ = 144.2°) 2991 independent reflections [R_{int} = 0.049], 210 parameters and 148 restraints, R_1 [for 2495 reflections with $I > 2\sigma(I)$] = 0.056 wR_2 (for all data) = 0.177, S = 1.05, largest diff. peak and hole = 0.27 e Å^{-3}/-0.23 e Å^{-3}.

2.12. Compound **8c**

$C_{15}H_{17}N_3O_4$, Mr = 303.32 g mol^{-1}, plates yellow, size = 0.16 × 0.12 × 0.02 mm, monoclinic, space group $P2_1/n$ (no.14), a = 14.6490 (9) Å, b = 7.0414 (5) Å, c = 15.5731 (10) Å, β = 115.737 (2)°, λ = 1.54178, Å V = 1447.00 (17) Å^3, Z = 4, D_{calcd} = 1.392 Mg m^{-3}, F(000) = 640, μ = 0.86 mm^{-1}, T = 173 K, 14391 measured reflections ($2\theta_{max}$ = 144.4°), 2838 independent reflections [R_{int} = 0.056], 206 parameters, 2 restraints, R_1 [for 2549 reflections with $I > 2\sigma(I)$] = 0.050, wR_2 (for all data) = 0.144, S = 1.04, largest diff. peak and hole = 0.32 e Å^{-3}/-0.32 e Å^{-3}.

2.13. Compound **8d**

$C_{15}H_{17}N_3O$ 1.5(H_2O), Mr = 314.34, g mol^{-1}, plates yellow, size = 0.35 0.25 × 0.20 mm, monoclinic, space group I (no.15), a = 17.8791 (3) Å, b = 11.1773 (2) Å, c = 16.4921 (2) Å, β = 100.178 (1)°, λ = 1.54178, Å V = 3243.92 (9) Å^3, Z = 8, D_{calcd} = 1.287 Mg m^{-3}, F(000) = 1336, μ = 0.80 mm^{-1}, T = 298 K, 16724 measured reflections ($2\theta_{max}$ = 144.4°), 3185 independent reflections [R_{int} = 0.056], 214 parameters, 169 restraints, R_1 [for 2799 reflections with $I > 2\sigma(I)$] = 0.069, wR_2 (for all data) = 0.215, S = 1.08, largest diff. peak and hole = 0.42 e Å^{-3}/-0.44 e Å^{-3}.

CCDC 2256765 (**8b**), 2256766 (**8c**), and 2256767 (**8d**) contain supplementary crystallographic data for this paper. These data can be obtained free of charge from The Cambridge Crystallographic Data Center *via* www.ccdc.cam.ac.uk/data_request/cif (deposited at the CSD April 17, 2023).

3. Results and discussion

To approach the synthesis of the targeted molecules, multi-synthetic steps had been carried out [27–29], as shown in Scheme 1. The reactions between 4-hydrazinylquinolin-2(1*H*)-ones **5a-g** and ethyl propiolate (**6**) were carried out in ethanol under refluxing conditions to afforded the corresponding 3-(2-(2-oxo-1,2-dihydroquinolin-4-yl)hydraz-ono)propanoate **8a-g** (Scheme 2). The reactions were prolonged under basic conditions to promote the cyclization to the pyrazole ring. Unfortunately, the reaction was proceed to without cycliziation and give the only open-chain products **8a-g** as a sole product.

The chemical composition of all the prepared compounds obtained are proved using modern spectroscopic methods such as: FTIR, ^{1}H NMR, ^{13}C NMR spectrum, mass spectrometry, elemental analysis, and as well as X-ray crystallography. Compound **8c** is selected as an example, which is assigned as (*E*)-ethyl 3-(2-(6-methoxy-2-oxo-1,2-dihydroquinolin-4-yl)hydrazono)propanoate (Fig. 3). The IR spectra of compound **8c**; have shown that the NH-group were observed at ν 3256 cm^{-1}. Moreover, an aromatic-CH stretching vibrated at ν 3085 cm^{-1}, and the aliphatic-CH at ν 2996 cm^{-1}. Also, other peaks appeared at ν 1727, 1638, and 1604 cm^{-1}, which assigned for (C═O ester), (C═O, quinolinone-C2), and C═N, respectively. The ^{1}H NMR spectra of compound **8c** showed four singlet signals at δ_H 3.80, 6.06, 7.52, 10.45, and 10.95 ppm, which were assigned as methoxy group, quinolinone-H-3, quinolone-H-5, hydrazone-NH and quinolinone-NH, respectively. The other characteristic signals for the ethyl group at δ_H 1.26 (t, J = 8.0 Hz, 3H, CH_3) and 4.14 ppm (q, J = 8.0 Hz, 2H, CH_2O). The presence of the ethyl group was confirmed from the ^{13}C NMR, which gives characteristic signals at δ_C 14.05 and 60.51 ppm for CH_3 and CH_2O- groups, respectively. Furthermore, two different carbonyl groups are resonated at δ_C 162.39 and 169.76 ppm, respectively, as quinolinone-C-2 and ester-CO. On the other hand, the mass spectrometry and elemental analysis confirmed that compound **8c** has a molecular formula $C_{15}H_{17}N_3O_4$ with m/z = 303, which confirmed that compound **8c** comes *via* interaction between 1 mol of 4-hydrazinyl-6-methoxyquinolin-2(1*H*)-one (**5c**) with 1 mol of ethyl propiolate (**6**) without any elimination as shown in Scheme 2.

Regarding the composition of ethyl propiolate (**6**), we notice that it contains two active centers, namely the carbonyl group (C═O) and the triple bond (C≡C); therefore, it is possible to form analogues of the compound during the intermediates **A**-**C**. If the reaction proceeded *via* intermediate **A**, the pyrazolylquinolin-2(1*H*)-ones **7a-g** would form; again, if the reaction proceeded through the intermediate **B**, our products **8a-g** and Z-form **9a-g** and pyrazolylquinolin-2(1*H*)-ones **10a-g**, would be obtained, but if the reaction proceeded through the intermediate **C**, the reaction would give the corresponding pyrazolylquinolin-2(1*H*)-ones **11a-g**. The possibility of forming these compounds is referred to as the stereoselectivity phenomena; the compounds **7a-g**, **10a-g,** and **11a-g** were ruled out at first sight according to ^{1}H NMR and ^{13}C NMR spectrum, in addition to the mass spectrometry. In addition, to distinguish between the two isomeric structures **8a-g** and **9a-g**, which comes from the reaction between 4-hydrazinylquinolin-2(1*H*)-ones **5a-c** and mole of ethyl propiolate (**6**) through the intermediate **B** as shown in Scheme 2.

The single crystals, suitable for X-ray measurements, were obtained from methanol. X-ray crystal structure analysis were performed for compound **8b**, **8c** and **8d** (see Figs. 4–6), which indicate that our obtained products as *E*-isomer as shown in Figs. 3–5. Geometrical

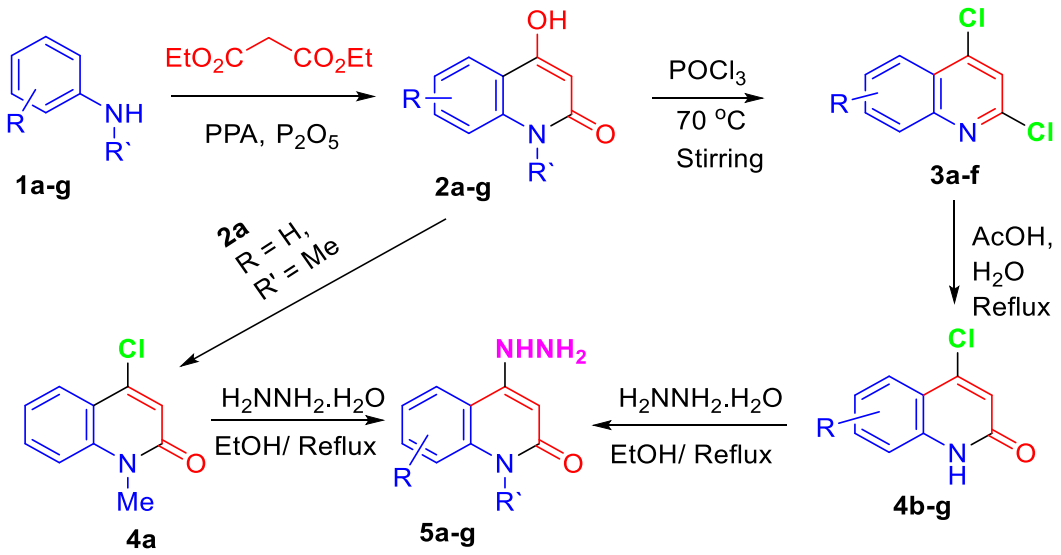

1,5: **a**, R = H, R` = Me; **b**, R = R` = H; **c**, R = 6-OMe, R` = H;
d, R = 6-Me, R` =H; **e**, R = 6-Cl, R` = H; f, R = 7-Me, R` = H;
g, R = 8-Me, R` =H

Scheme 1. Strategy for the synthesis of hydrazonoquinolone **5a-g**.

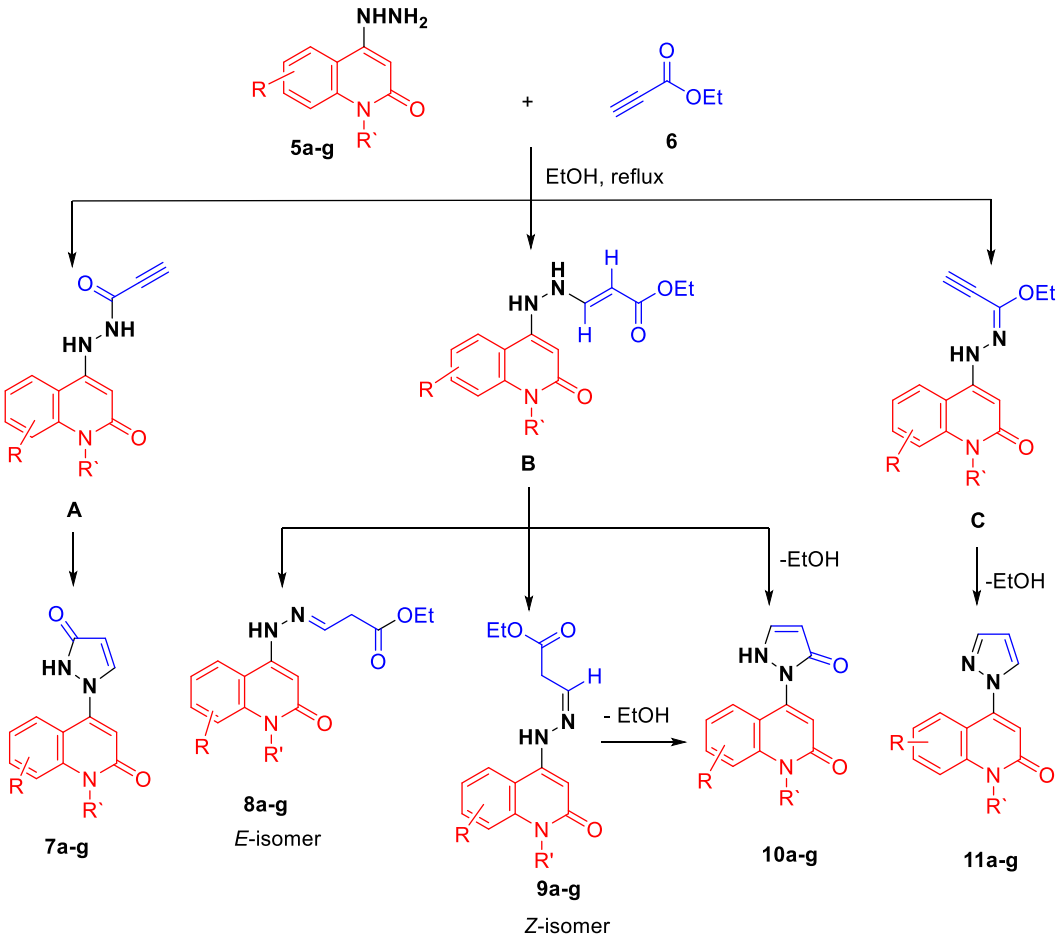

5 and 7-11a-g: **a**, R = H, R` = Me; **b**, R = R` = H; **c**, R = 6-OMe, R` = H; **d**, R = 6-Me, R` = H; **e**, R = 6-Cl, R` = H; **f**, R = 7-Me, R` = H; **g**, R = 8-Me, R` =H

Scheme 2. Stereoselective interaction of hydrazinylquiolinone **5a-g** with ethyl propiolate **6** and synthesis of 1,2-dihydroquinolinehydrazonopropanoate derivatives **8a-g**.

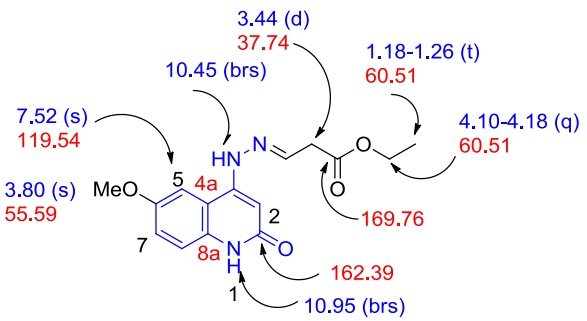

Fig. 3. Chemical structure for (*E*)- ethyl 3-(2-(6-methoxy-2-oxo-1,2-dihydroquinolin-4-yl)hydrazinylidene)propanoate (**8c**).

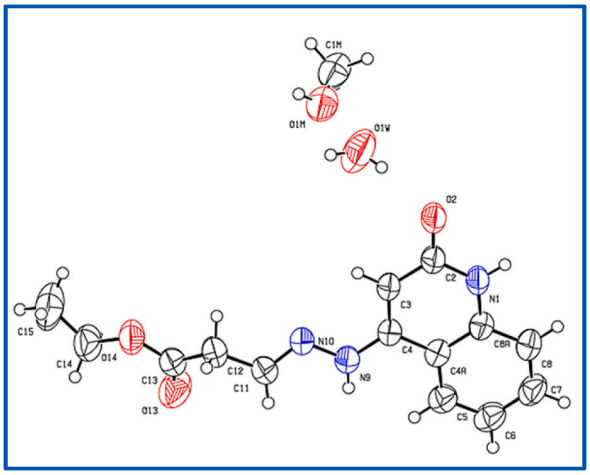

Fig. 4. X-Ray crystallographic molecular structure for (*E*)-ethyl 3-(2-(2-oxo-1,2-dihydroquinolin-4-yl)hydrazono)propanoate (**8b**) (solvent omitted for clarity, displacement parameters are drawn at 30 % probability level).

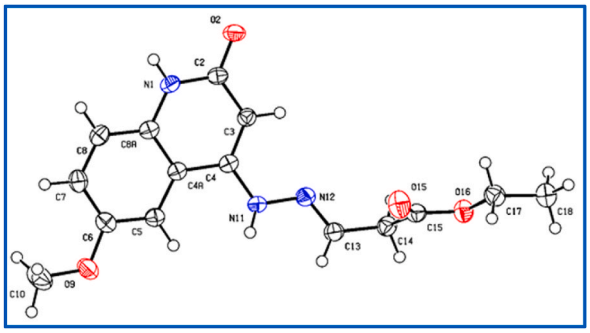

Fig. 5. X-Ray crystallographic molecular structure for (*E*)-ethyl 3-(2-(6-methoxy-2-oxo-1,2-dihydroquinolin-4-yl)hydrazono)propanoate (**8c**) (displacement parameters are drawn at 50 % probability level).

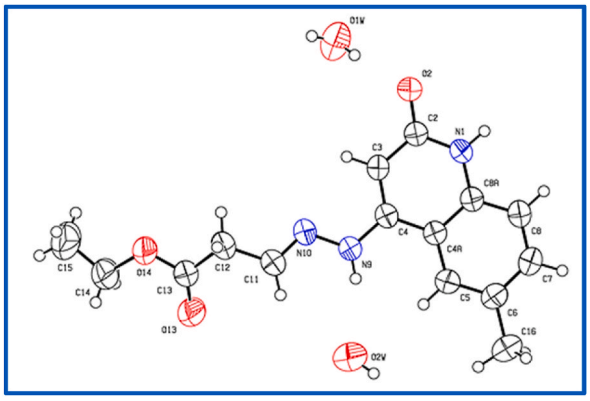

Fig. 6. X-Ray crystallographic molecular structure for (*E*)-Ethyl 3-(2-(6-methyl-2-oxo-1,2-dihydroquinolin-4-yl)hydrazono)propanoate (**8d**) (solvent omitted for clarity, displacement parameters are drawn at 30 % probability level).

parameters are in the expected range for 1,2-dihydroquinolin-4-yl)hydrazono)propanoate (see Table 1). The 1,2dihydroquinoline and the hydrazono moieties are slightly twisted (7.4° (**8b**), 15.5° (**8c**), 8.3° (**8d**), see Table 1].

The X-ray data of compound **8c** proves that (*E*)-ethyl 3-(2-(6-methyl-2-oxo-1,2-dihydroquinolin-4-yl)hydrazono)propanoate was formed exclusively from the reaction of **8c** with ethyl propiolate. All the X-ray structure confirmed the *E*-configuration concerning

Table 1
Selected bond distances [Å], bond angles [°] and dihedral angles [°] for **8b**, **8c** and **8d** [in brackets for **8c**].

[in brackets for 8c]	8b	8c	8d
N1–C2	1.362(2)	1.3635(18)	1.354(2)
N1–H1	0.86	0.870(15)	0.86
C2–O2	1.259(2)	1.2628(17)	1.261(2)
C2–C3	1.421(2)	1.4255(19)	1.423(3)
C3–C4	1.364(2)	1.3627(19)	1.371(3)
C4–C4a	1.455(2)	1.4558(19)	1.445(2)
C4a-C8a	1.407)2)	1.411(2)	1.404(3)
N1–C8a	1.381(2)	1.3816(19)	1.381(3)
C4–N9 [C4–N11]	1.366(2)	1.3824(18)	1.377(2)
N9–N10 [N11–N12]	1.375(2)	1.3753(16)	1.366(2)
N9–H9 [N11–H11]	0.86	0.876(14)	0.86
N10–C11 [N12–C13]	1.261(2)	1.2659(19)	1.263(3)
C11–C12 [C13–C14]	1.490(2)	1.4966(19)	1.494(3)
C4–N9–N10 [C4–N11–N12]	118.85(14)	117.20(11)	118.25(15)
N9–N10–C11 [N11–N12–C13]	117.38(15)	115.86(12)	117.45(17)
N10–C11–C12 [N12–C13–C14]	119.44(17)	118.54(13)	118.47(19)
C3–C4–N9–N10 [C3–C4–N11–N12]	−1.8(3)	−1.1(2)	−5.0(3)
C4a-C4-N9-N10 [C4a-C4-N11-N12]	177.51(15)	178.63(11)	174.41(17)
C4–N9–N10–C11 [C4–N11–N12–C13}	−169.71(18)	156.97(13)	−170.8(2)
N9–N10–C11–C12 [N11–N12–C13–C14]	−179.37(17)	179.67(12)	−179.88(19)
angle between the normal of the l.S. planes of the 1,2dihydroquinoline and the hydrazono moiety [°]	7.4	15.5	8.3

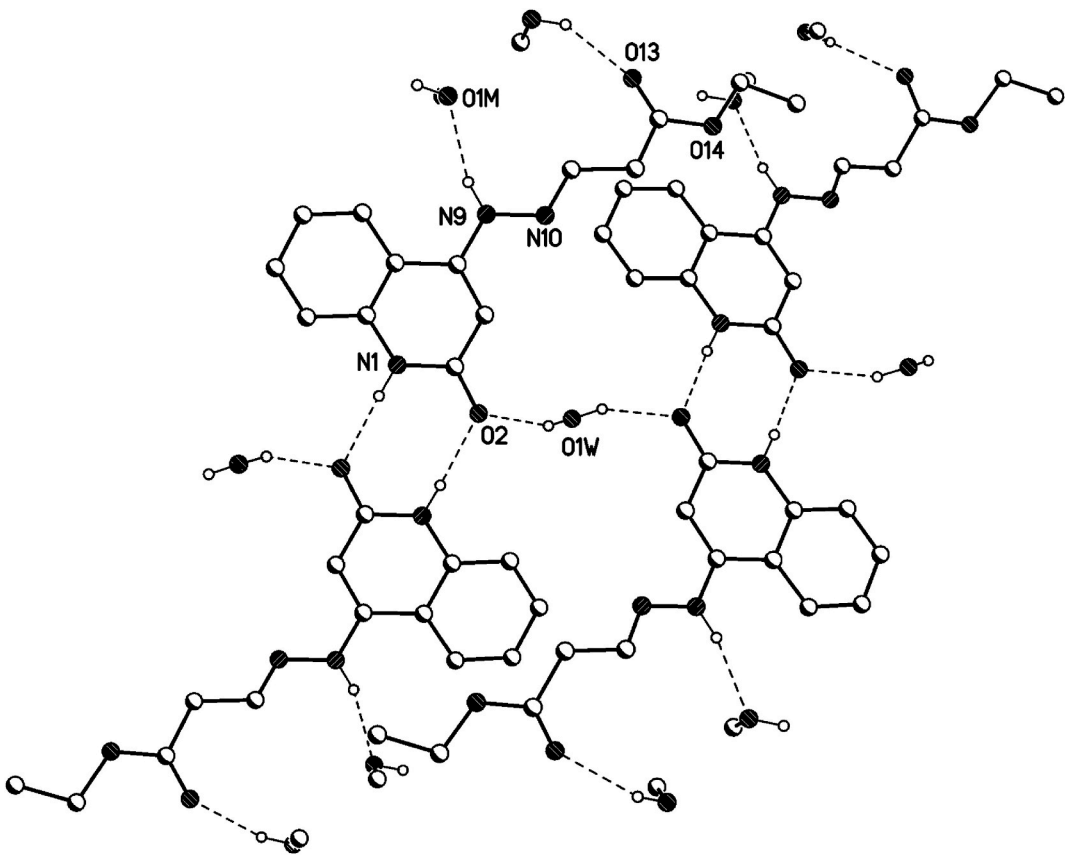

Fig. 7. Intermolecular hydrogen bonds of compound **8b** showing hydrogen bonds as dashed lines.

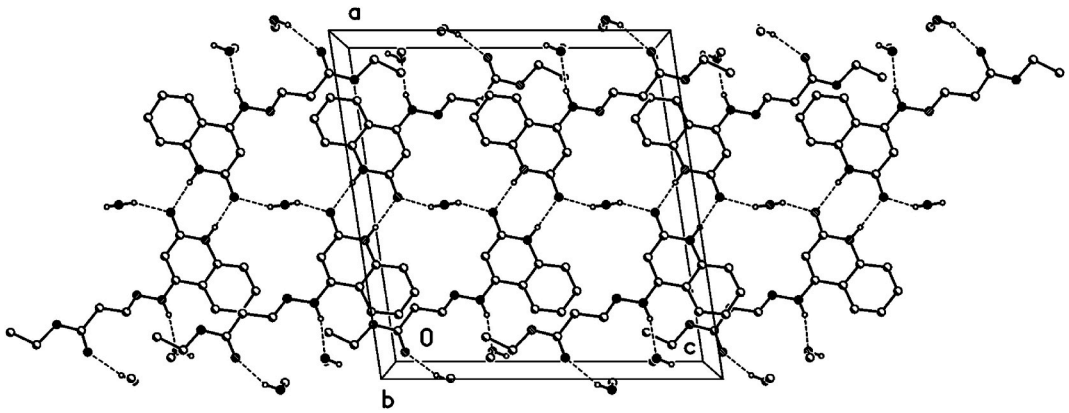

Fig. 8. Crystal packing of compound **8b** showing hydrogen bonds as dashed lines.

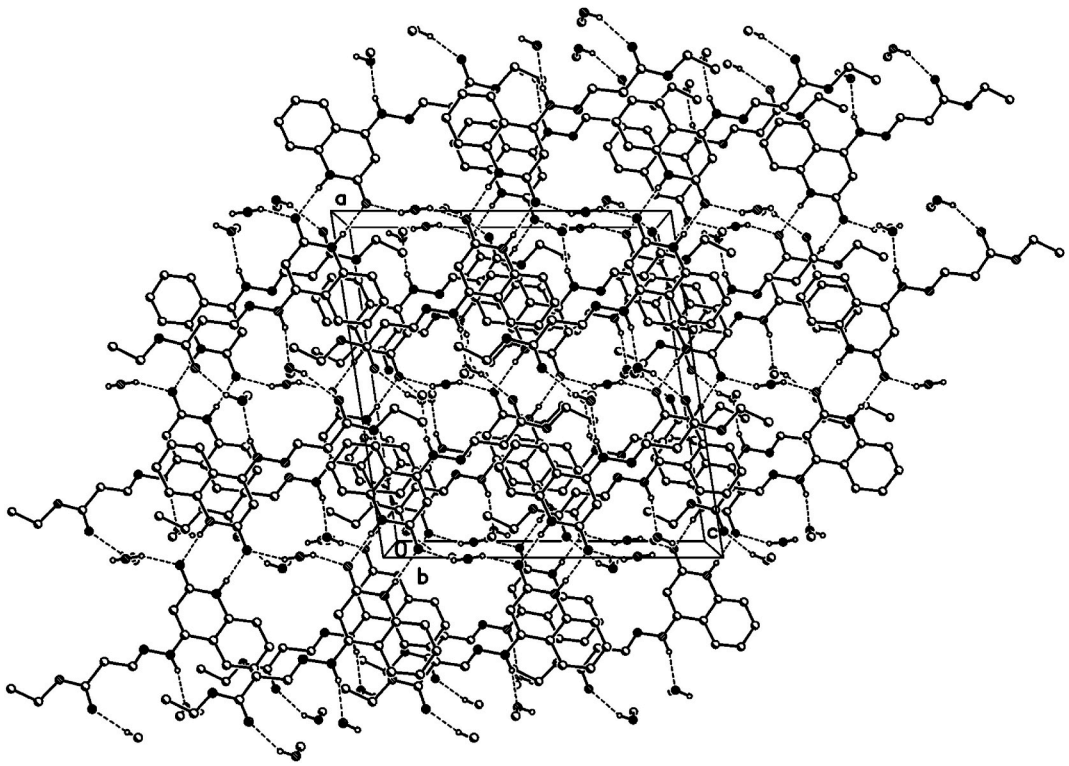

Fig. 9. Crystal packing of compound **8b** showing hydrogen bonds as dashed lines.

Table 2
Selected hydrogen-bond geometry (Å, °) for **8b**.

D—H···*A*	*D*—H	H···*A*	*D*···*A*	*D*—H···*A*
N1–H1···O2^{i}	0.86	1.98	2.836 (2)	175
N9–H9···O1*M*^{ii}	0.86	2.07	2.900 (3)	162
O1*M*—H1*M*···O13^{iii}	0.82	2.19	2.823 (3)	135
O1*W*–H1*W*···O2	0.82 (1)	1.93 (3)	2.699 (2)	155 (5)

Symmetry codes: (i) -*x*+1, -*y*+1, -*z*+2; (ii) -*x*+1/2, *y*+1/2, -*z*+3/2; (iii) *x*+1/2, *y*-1/2, *z*.

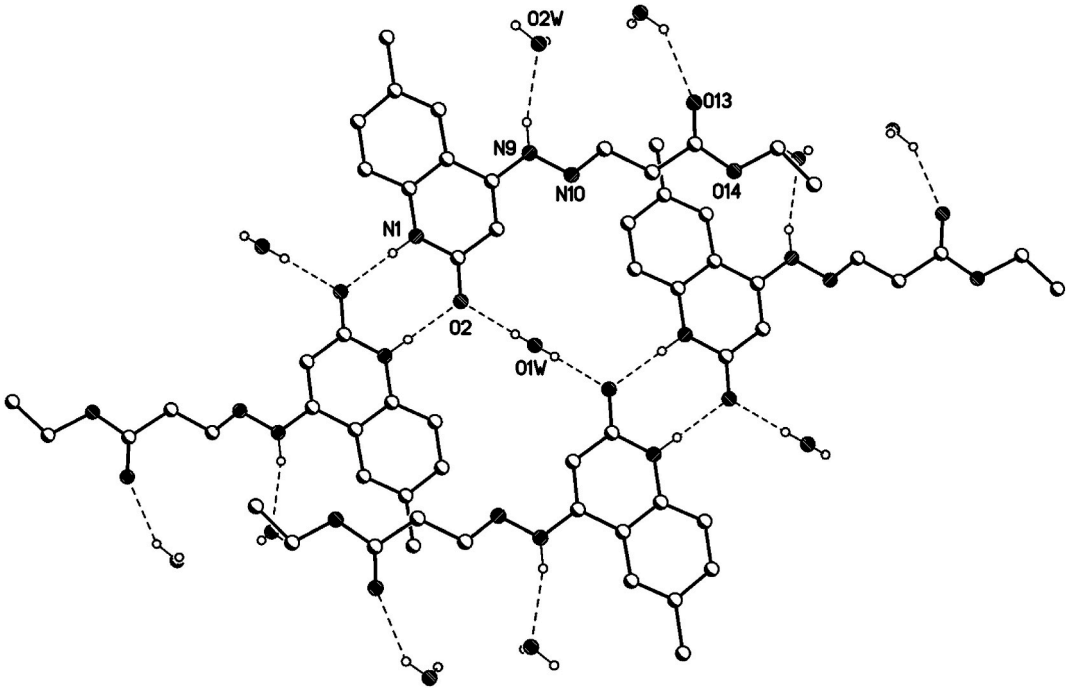

Fig. 10. Intermolecular hydrogen bonds of compound **8d** showing hydrogen bonds as dashed lines.

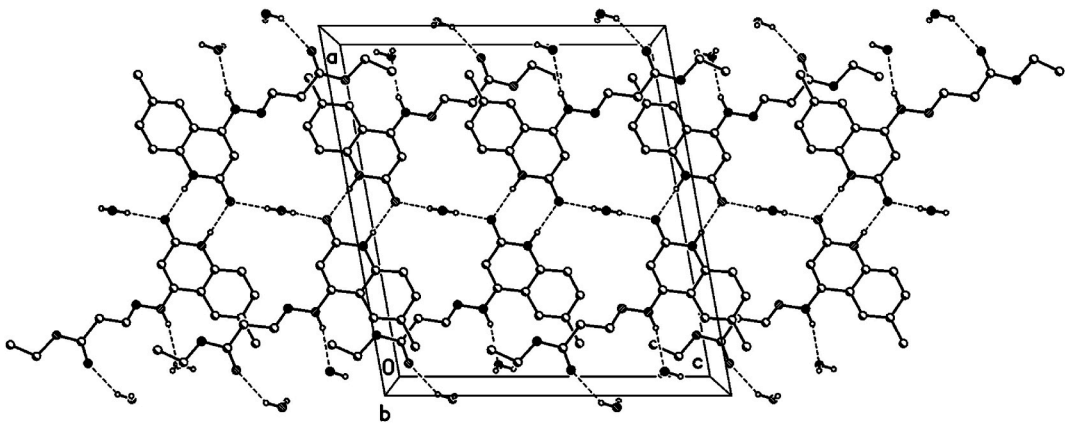

Fig. 11. Crystal packing of compound **8d** showing hydrogen bonds as dashed lines.

N10=C11 (**8b**, **8d**), N12=C13 (**8c**). As outlined from the X-ray structure, the configuration of all compounds in the *E*-form shows that pyrazole does not form because the *E*-form makes the electrophilic site far from the attack of the nucleophilic hydrazine-N[1].

The crystal packing of **8b**, **8c** and **8d** shows intermolecular hydrogen bonds as well as π-π interactions.

3.1. Intermolecular hydrogen bonds for 8b, 8c and 8d

All three compounds form centrosymmetric dimers *via* intermolecular hydrogen bonds (N1–H1···O2). There are additional intermolecular hydrogen bond for **8b** and **8d** with the disordered solvent (MeOH for **8b** and water for **8d**) for N9–H9···O(solvent) and O–H(solvent)…O13. In addition, **8b** and **8d** are intermolecular hydrogen bonds *via* the ordered water molecule (O1W on special position at the 2-fold axis, O1W–H1W···O2) linking the dimers. For **8c**, there are additional intermolecular hydrogen bonds C13–H13···O2, N11–H11···O2 (see details below) [33–35].

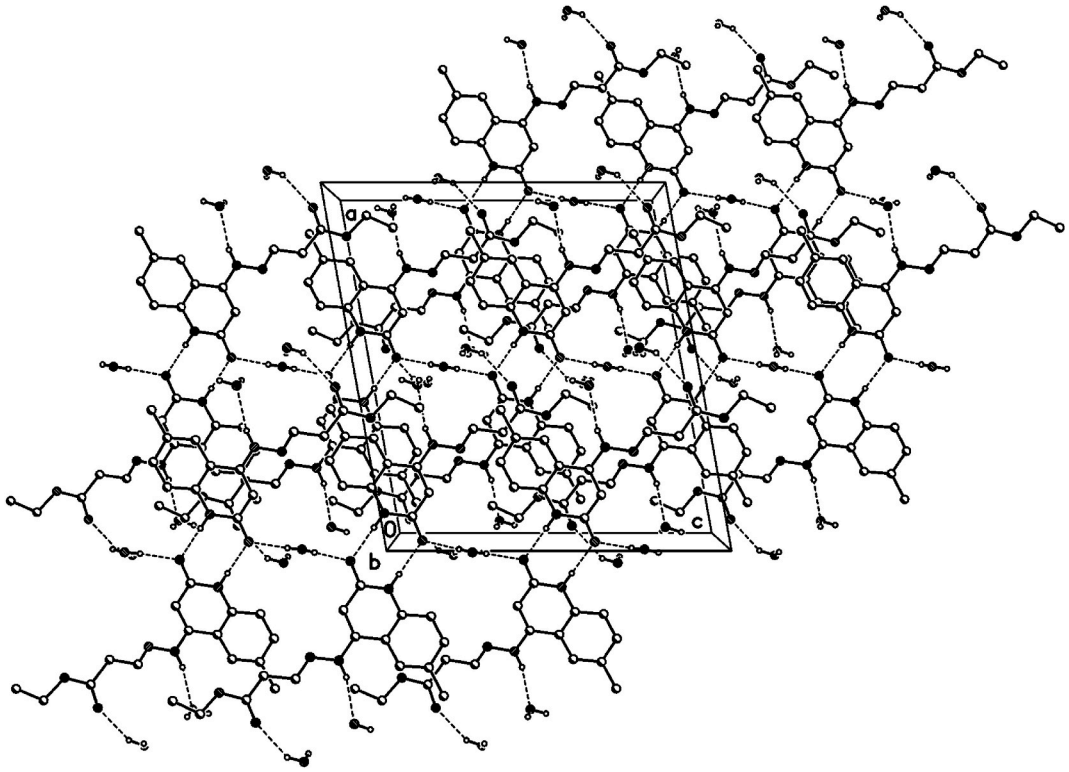

Fig. 12. Crystal packing of compound **8d** showing hydrogen bonds as dashed lines.

Table 3
Selected hydrogen-bond geometry (Å, °) for **8d**.

D—H···*A*	*D*—H	H···*A*	*D*···*A*	*D*—H···*A*
N1–H1···O2^{i}	0.86	1.98	2.839 (2)	178
N9–H9···O2*W*	0.86	2.20	3.044 (3)	165
O1*W*–H1*W*···O2	0.83 (1)	1.94 (2)	2.736 (2)	163 (5)
O2*W*–H2*W*1···O13^{ii}	0.82 (1)	2.20 (5)	2.914 (3)	146 (7)

Symmetry codes: (i) -*x*+1, -*y*+1, -*z*+2; (ii) -*x*, *y*, -*z*+3/2.

3.2. Hydrogen bonds 8b

In the crystal packing of **8b** (Figs. 7–9), the molecules are linked by intermolecular N9–H9···O1M, O1M-H1M···O13, O1W–H1W···O2, and N1–H1···O2 hydrogen bonds (Table 2) in a two-dimensional network parallel to the ac plane. The MeOH solvent molecule is disordered about a 2-fold axis (symmetry operator 1-x, y, 1.5-z), there is half a MeOH molecule in the asymmetric unit (or 0.5 MeOH molecule per formula moiety).

3.3. Hydrogen bonds 8d

In the crystal packing of **8d** (Figs. 10–12), the molecules are linked by intermolecular N9–H9···O2W, O2W–H2W1···O13, O1W–H1W···O2, and N1–H1···O2 hydrogen bonds (Table 3) in a two-dimensional network parallel to the ac plane. In 4 voids are 8 solvent water molecules (2 per void generated about a 2-fold axis (symmetry operator -x, y, 1.5-z, one water molecule per formula moiety). These water molecules are probably disordered.

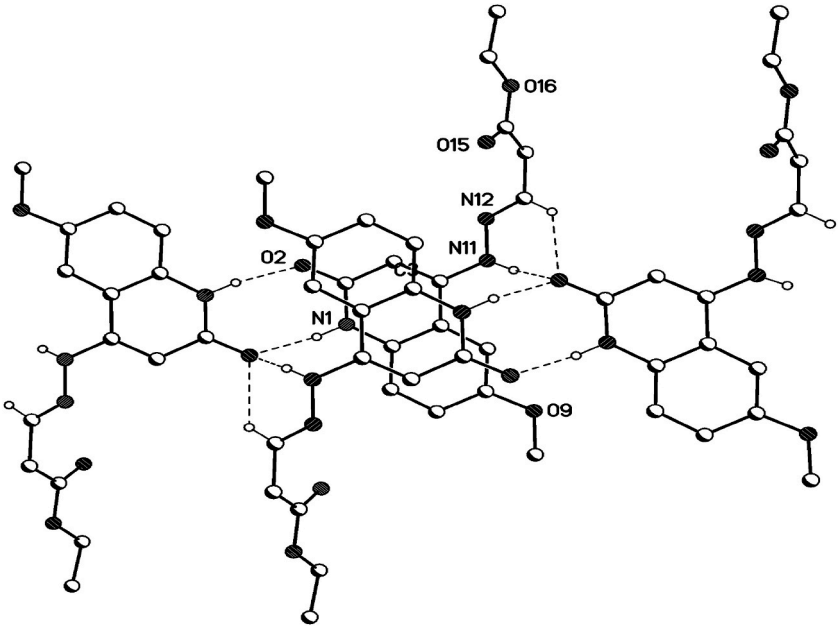

Fig. 13. Intermolecular hydrogen bonds of compound **8c** showing hydrogen bonds as dashed lines.

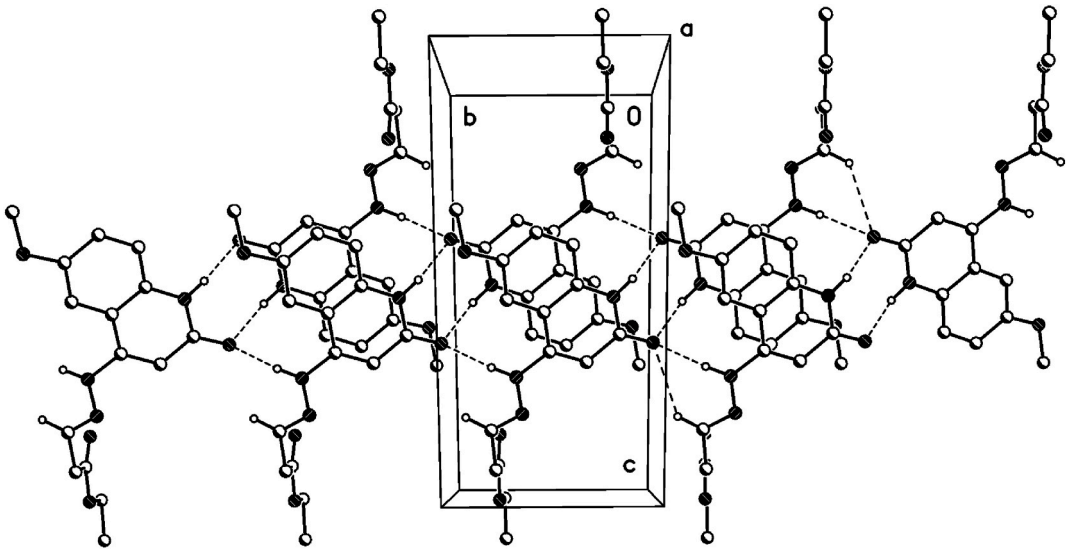

Fig. 14. Crystal packing of compound **8c** showing hydrogen bonds as dashed lines.

3.4. Hydrogen bonds 8c

In the crystal packing of **8c** (Figs. 13–15), the molecules are linked by intermolecular C13–H13···O2, N11–H11···O2, and N1–H1···O2 hydrogen bonds (Table 4) There are dimers in the b/c plane which are linked by bifurcular hydrogen bonds (C13–H13···O2, N11–H11···O2) forming an one-dimensional network along the a-axis, as well as π···π interactions along the a-axis (see below).

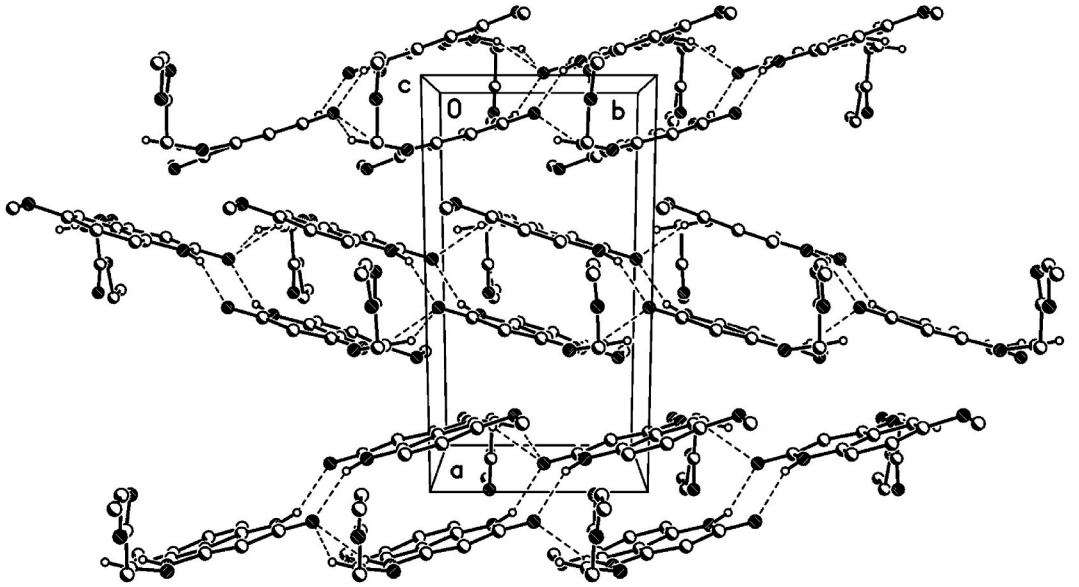

Fig. 15. Crystal packing of compound **8c** showing hydrogen bonds as dashed lines.

Table 4
Selected hydrogen-bond geometry (Å, °) for **8c**.

D—H···*A*	*D*—H	H···*A*	*D*···*A*	*D*—H···*A*
N1–H1···O2^{i}	0.87 (2)	2.01 (2)	2.8219 (16)	154 (2)
N11–H11···O2^{ii}	0.88 (1)	2.08 (2)	2.9003 (16)	155 (2)
C13–H13···O2^{ii}	0.95	2.60	3.3397 (18)	135

Symmetry codes: (i) -*x*+1, -*y*+2, -*z*+1; (ii) *x*, *y*-1, *z*.

Table 5
Geometrical parameters for the π-stacking moieties involved in the π···π interactions [Å, °] (Cg1 centroid of the ring N1–C2–C3–C4–C4a-C8a, Cg2 centroid of the ring C4a-C5-C6-C7-C8-C8a).

Compound	8b	8d	8c
centroid distance between Cg1…C2ga/Cg2…Cg1a	4.04	4.38	3.50
Vertical distance from ring centroids Cg1/Cg2 to symmetry related 1,2-dihydroquinolin	3.42	3.52	3.38
angle between the centroid vector Cg1…C2ga/Cg2…Cg1a and the normal to the 1,2-dihydroquinolin plane	147.9 (32.1)	143.3 (36.7)	165.0 (25.0)
symmetry operator (a)	0.5-x, 1.5-y, 2-z	0.5-x, 1.5-y, 2-z	1-x, 1-y, 1-z

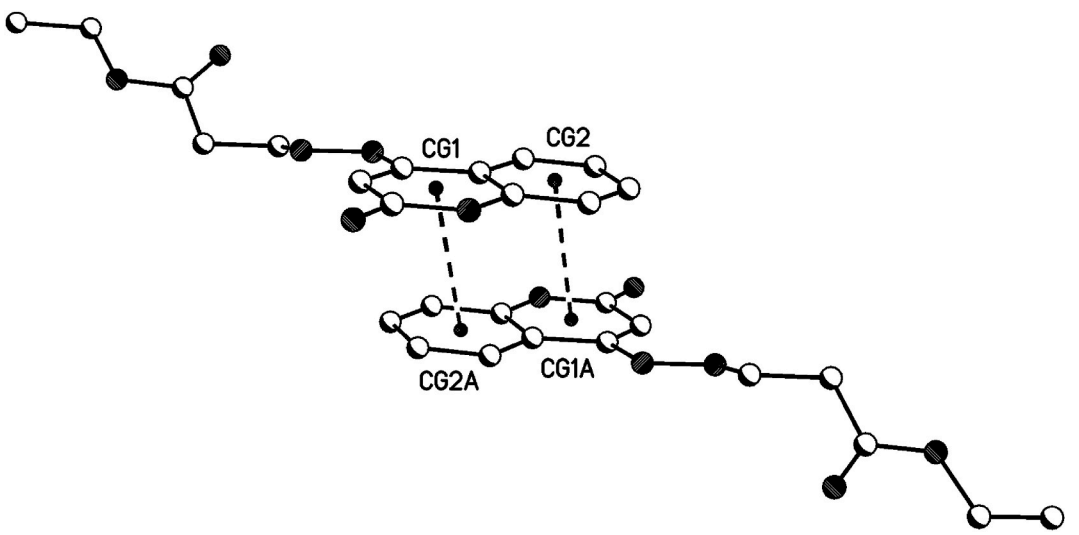

Fig. 16. π···π interactions of compound **8b** (solvent and hydrogen atoms omitted for clarity).

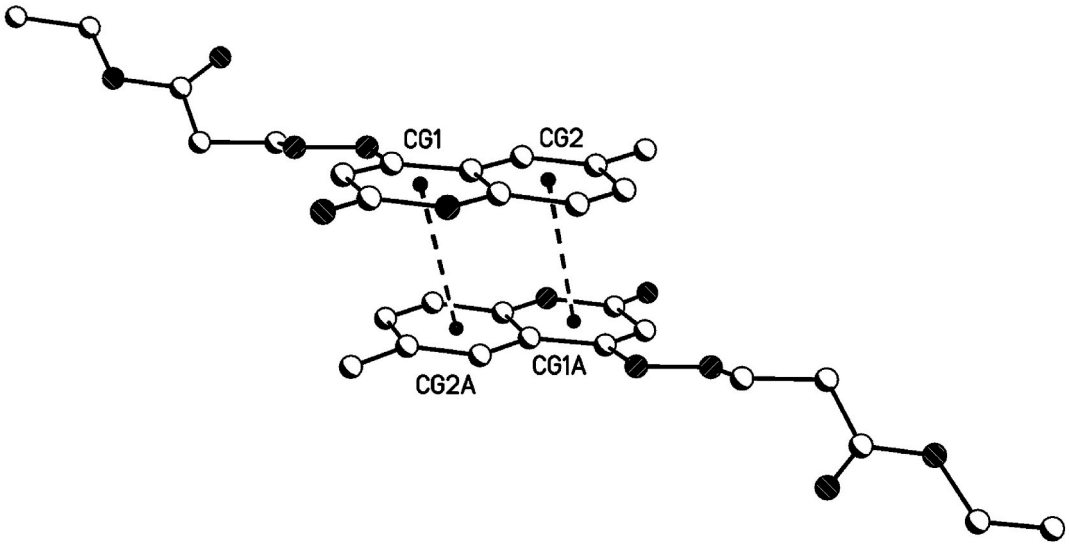

Fig. 17. π···π interactions of compound **8d** (solvent and hydrogen atoms omitted for clarity).

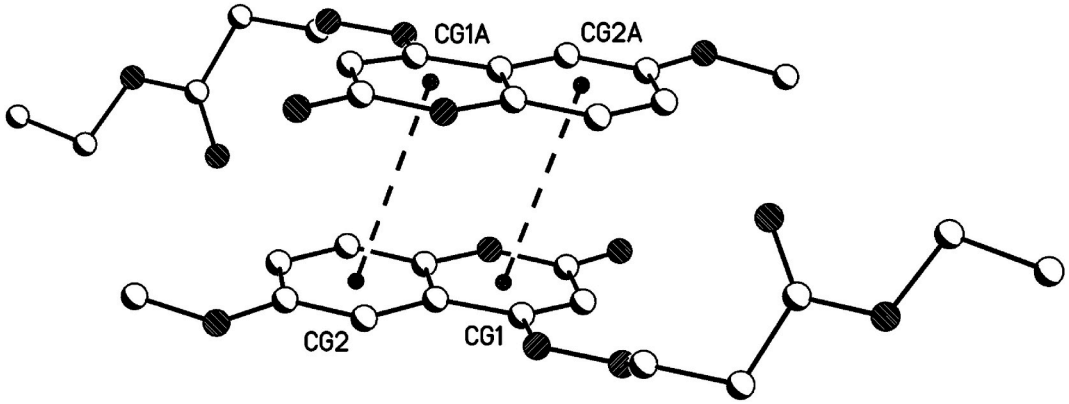

Fig. 18. π···π interactions of compound **8c** (solvent and hydrogen atoms omitted for clarity).

3.5. π···π interactions

For 1,2-dihydroquinoline moieties in all 3 compounds **8b**, **8c** and **8d**, centrosymmetric dimers are generated by π···π interactions (see Table 5, Figs 16–18). In **8b** and 8d, these dimers linked the 2D-hydrogen bond networks in the a/c plane by π···π interactions in the direction of the b-axis. In **8c**, these dimers linked the hydrogen bonded dimers in the b/c plane by π···π interactions in the direction of the a-axis (see also the 1D hydrogen bond network along the a-axis).

The symmetry related planes of the 1,2-dihydroquinolin dimers are coplanar (centrosymmetric symmetry operator, see Table 5). Therefore, the angel between the symmetry related 1,2-dihydroquinolins are 0°.

Based on the (*E*)-configuration of the products as attempted by X-ray crystallographic determination, the plausible mechanism of the nucleophilic addition reaction (1,4-addition) which is mentioned as aza-Michael addition as mentioned in Scheme 3. The mechanism involved two main nucleophilic additional steps; on each step, the nucleophilic attack occurs *via* the lone pairs of electrons on the hydrazine nitrogen (N^2), and the final product was obtained through the formation of intermediates **12–15**. The steps of the mechanism involved two transformation of *enol*-form to *keto*-form structures: intermediate **13** (enol-form) to intermediate-**B** (keto-form) and intermediate **15** (enol-form) to the final product **8a** as the more stable keto-form.

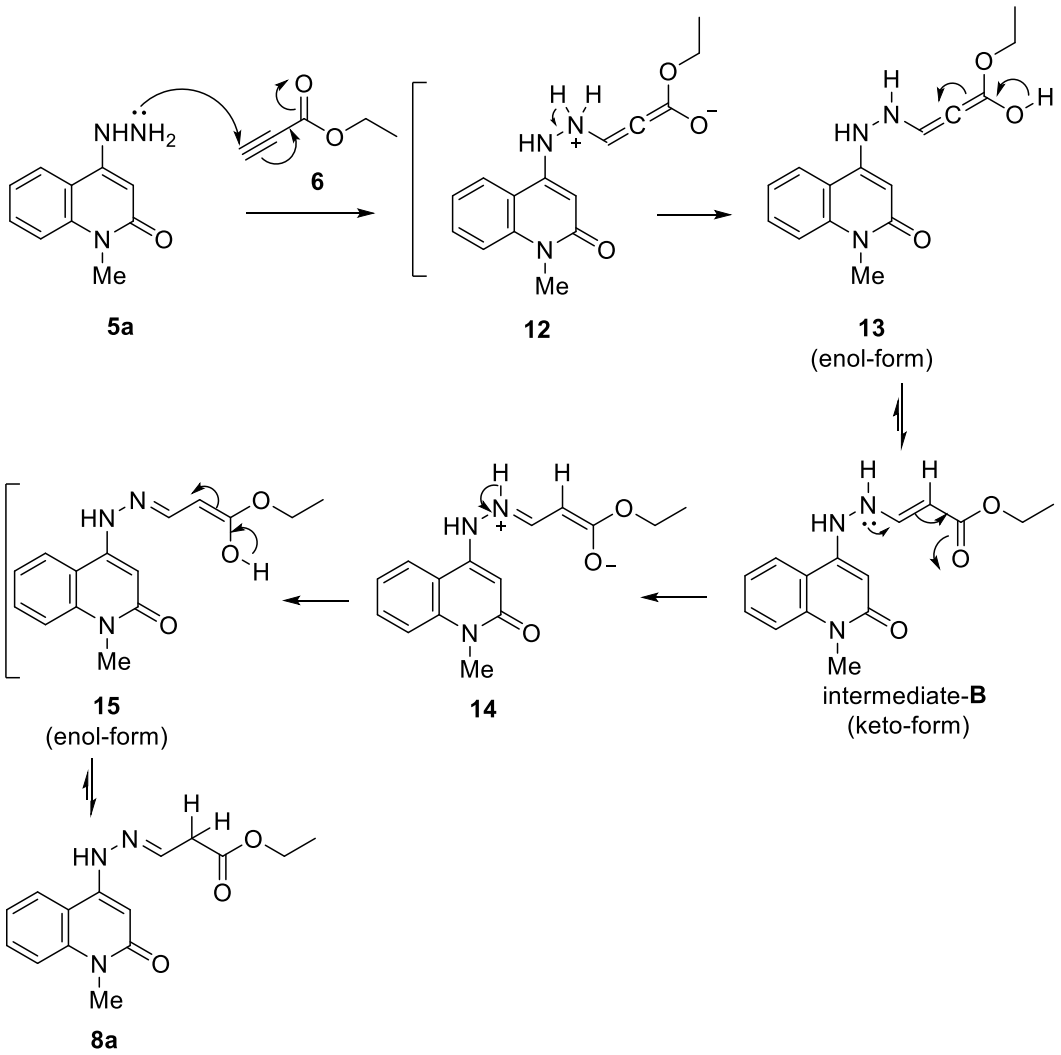

Scheme 3. Postulated mechanism for the formation of compound **8a** ((*E*)-1-methyl-4-(2-(3-oxohexylidene)hydrazinyl)quinolin-2(1*H*)-one).

4. Conclusion

We have reported in this article the synthesis of ethyl hydrazonoquinolone propanoate derivatives *via* a convenient reaction between substituted hydrazinyl-quinolinones and ethyl propiolate and determined the structure using advanced techniques of analyses and confirmed the correct structure using X-ray crystallographic analysis. Also, the X-ray discussion of the hydrogen bond among the molecules, as well as the pi-pi stacking interaction in the crystallatice.

Data availability statement

Data associated with the study has not been deposited into a publicly available repository. Data will be made available on request.

CRediT authorship contribution statement

Hendawy N. Tawfeek: Writing – original draft, Methodology, Conceptualization. **Ahmed M. Tawfeek:** Project administration. **Stefan Bräse:** Writing – review & editing, Formal analysis. **Martin Nieger:** Writing – review & editing, Formal analysis, Data curation. **Essmat M. El-Sheref:** Writing – review & editing.

Declaration of competing interest

No conflict of interest exists.

All authors confirm that there are no known conflicts of interest associated with this publication and there has been no significant financial support for this work that could have influenced its outcome.

Dr. Hendawy N. Tawfeek (Corresponding author) hendawy1976@yahoo.com.

Acknowledgments

Authors highly appreciate the financial support through researchers supporting the Project No. RSPD2024R672, King Saud University Riyadh, Saudi Arabia. Also, we acknowledge support by the KIT-Publication Fund of the Karlsruhe Institute of Technology, Karlsruhe, Germany.

Appendix A. Supplementary data

Supplementary data to this article can be found online at https://doi.org/10.1016/j.heliyon.2024.e25248.

References

[1] A. Bessonova, Components of *Haplophyllum bucharicum*, Chem. Nat. Compd. 36 (2000) 323–324, https://doi.org/10.1007/BF02238348.
[2] A. Detsi, V. Bardakaos, J. Markopoulos, Reactions of 2-methyl-3,1-benzoxazin-4-one with active methylene compounds: a new route to 3-substituted 4-hydroxyquinolin-2(1*H*)-ones, J. Chem. Soc. Perkin. Trans. 1 (1996) 2909–2913, https://doi.org/10.1039/p19960002909.
[3] V.I. Ukrainets, I.N. Bereznyakova, V.E. Mospanova, 4-Hydroxy-2-quinolones 121. Synthesis and biological properties of 1-hydroxy-3-oxo-5,6-dihydro-3h-pyrrolo[3,2,1-*ij*]quinoline-2-carboxylic acid alkylamides, Chem. Heterocycl. Compd. 43 (2007) 856–862, https://doi.org/10.1007/s10593-007-0136-4.
[4] M. Mizuta, H. Kanamori, Mutagenic activities of dictamnine and gamma-fagarine from dictamni radicis cortex (Rutaceae), Mutat. Res. Lett. 144 (1985) 221–225, https://doi.org/10.1016/0165-7992(85)90054-5.
[5] V. Duraipandiyan, S. Ignacimuthu, Antibacterial and antifungal activity of Flindersine isolated from the traditional medicinal plant, *Toddalia asiatica* (L.) Lam, J. Ethnopharmacol. 123 (2009) 494–498, https://doi.org/10.1016/jjep200902020.
[6] A. Debbab, A.H. Aly, W.H. Lin, P. Proksch, Bioactive compounds from marine bacteria and fungi, Microb. Biotechnol. 3 (2010) 44–563, https://doi.org/10.1111/j.1751-7915.2010.00179.x.
[7] J. Konieczny, K. Ossowska, G. Schulze, H. Coper, S. Wolfarth, L-701,324, a selective antagonist at the glycine site of the NMDA receptor, counteracts haloperidol-induced muscle rigidity in rats, Psychopharmacology (Berl) 143 (1999) 235–243, https://doi.org/10.1007/s002130050942.
[8] D. Dhanak, K. Duffy, V.K. Johnston, J. Lin-Goerke, M. Darcy, A.N. Shaw, G. Baohua, C. Silverman, A.T. Gates, D.L. Earnshaw, D.J. Casper, A. Kaura, A. Baker, C. Greenwood, L.L. Gutshall, D. Maley, A. DelVecchio, R. Macarron, G.A. Hofmann, Z. Alnoah, H.-Y. Cheng, G. Chan, S. Khandekar, R.M. Keenan, R.T. Sarisky, Identification and biological characterization of heterocyclic inhibitors of the hepatitis C virus RNA-dependent RNA polymerase, J. Biol. Chem. 277 (2002) 38322–38327, https://doi.org/10.1074/jbc.m205566200.
[9] D. Douche, Y. Sert, S.A. Brandán, A.A. Kawther, B. Bilmez, N. Dege, A.E. Louzi, K. Bougrin, K. Karrouchi, B. Himmi, 5-((1H-imidazole-1-yl)methyl)quinolin-8-ol as potential antiviral SARS-CoV-2 candidate: synthesis, crystal structure, Hirshfeld surface analysis, DFT and molecular docking studies, J. Mol. Struct. 1232 (2021) 130005, https://doi.org/10.1016/j.molstruc.2021.130005, 2021 May 15.
[10] O.O. Ajani, C.A. Obafemi, O.C. Nwinyi, D.A. Akinpelu, Microwave-assisted synthesis and antimicrobial activity of 2-quinoxalinone-3-hydrazone derivatives, Bioorg. Med. Chem. 18 (2010) 214–221, https://doi.org/10.1016/j.bmc.2009.10.064.
[11] P. Melnyk, V. Leroux, C. Sergheraert, P. Grellier, Design, synthesis and in vitro antimalarial activity of an acylhydrazone library, Bioorg. Med. Chem. Lett. 16 (2006) 31–35, https://doi.org/10.1016/j.bmcl.2005.09.058.
[12] L.W. Zheng, L.L. Wu, B.X. Zhao, W.L. Dong, J.Y. Miao, Synthesis of novel substituted pyrazole-5-carbohydrazide hydrazone derivatives and discovery of a potent apoptosis inducer in A549 lung cancer cells, Bioorg. Med. Chem. 17 (2009) 1957–1962, https://doi.org/10.1016/j.bmc.2009.01.037.
[13] K.A. Metwally, L.M. Abdel-Aziz, E.S.M. Lashine, M.I. Husseiny, R.H. Badawy, Hydrazones of 2-aryl-quinoline-4-carboxylic acid hydrazides: synthesis and preliminary evaluation as antimicrobial agents, Bioorg. Med. Chem. 14 (2006) 8675–8682, https://doi.org/10.1016/j.bmc.2006.08.022.
[14] S. Eswaran, A.V. Adhikari, N.K. Pal, I.H. Chowdhury, Design and synthesis of some new quinoline-3-carbohydrazone derivatives as potential antimycobacterial agents, Bioorg. Med. Chem. Lett. 20 (2010) 1040–1044, https://doi.org/10.1016/j.bmcl.2009.12.045.
[15] A. Nayyar, V. Monga, A. Malde, E. Coutinho, R. Jain, Synthesis, anti-tuberculosis activity, and 3D-QSAR study of 4-(adamantan-1-yl)-2-substituted quinolines, Bioorg. Med. Chem. 15 (2007) 626–640, https://doi.org/10.1016/j.bmc.2006.10.064.
[16] K.D. Thomas, A.V. Adhikari, S. Telkar, I.H. Chowdhury, R. Mahmood, N.K. Pal, G. Row, E. Sumesh, Design, synthesis and docking studies of new quinoline-3-carbohydrazide derivatives as anti-tubercular agents, Eur. J. Med. Chem. 46 (2011) 5283–5292, https://doi.org/10.1016/j.ejmech.2011.07.033.
[17] S. Kumar, S. Bawa, S. Drabu, R. Kumar, L. Machawal, Synthesis and in vivo anti-convulsant evaluation of 2-chloroquinolinyl hydrazone derivatives, Acta. Pol. Pharmaceutica-Drug Research 67 (2010) 567–573. https://pubmed.ncbi.nlm.nih.gov/20873428/.
[18] L.V. Reddy, S.B. Nallapati, S.S. Beevi, L.N. Mangamoori, K. Mukkanti, S.A. Pal, A "green" synthesis of N-(quinoline-3-ylmethylene)benzohydrazide derivatives and their cytotoxicity activities, J. Braz. Chem. Soc. 22 (2011) 1742–1749, https://doi.org/10.1590/S0103-50532011000900017.
[19] M. Arıcı, O.Z. Yeşilel, E. Acar, N. Dege, Synthesis, characterization and properties of nicotinamide and isonicotinamide complexes with diverse dicarboxylic acids, Polyhedron 127 (2017) 293–301, https://doi.org/10.1016/j.poly.2017.02.013.
[20] M. Bingul, O. Tan, C.R. Gardner, S.K. Sutton, G.M. Arndt, G.M. Marshall, B.B. Cheung, N.K. David, StC. Black, synthesis, characterization and anti-cancer activity of hydrazide derivatives incorporating a quinoline moiety, Molecules 21 (2016) 916–935, https://doi.org/10.3390/molecules21070916.
[21] M.A.I. Elbastawesy, Y.A.M.M. El-Shaier, M. Ramadan, A.B. Brown, A.A. Aly, G. El-D, A. Abuo-Rahma, Identification and molecular modeling of new quinolin-2-one thiosemicarbazide scaffold with antimicrobial urease inhibitory activity, Mol. Divers. 25 (2021) 13–27, https://doi.org/10.1007/s11030-019-10021-0.
[22] J. Valencia, V. Rubio, G. Puerto, L. Vasquez, A. Bernal, J.R. Mora, S.A. Cuesta, J.L. Paz, B. Insuasty, R. Abonia, J. Quiroga, A. Insuasty, A. Coneo, O. Vidal, E. Márquez, D. Insuasty, QSAR studies, molecular docking, molecular dynamics, synthesis, and biological evaluation of novel quinolinone-based thiosemicarbazones against, Mycobacterium Tuberculosis. Antibiotics 12 (2023) 61–91, https://doi.org/10.3390/antibiotics12010061.
[23] M.A.I. Elbastawesy, A.A. Aly, M. Ramadan, Y.A.M.M. Elshaier, B.G.M. Youssif, A.B. Brown, G.E.A. Abuo-Rahma, Novel pyrazoloquinolin-ones: design, synthesis, docking studies, and biological evaluation as antiproliferative EGFR- TK inhibitors, Bioorg. Chem. 90 (2019) 103045–103060, https://doi.org/10.1016/j.bioorg.2019.103045.
[24] L.H. Al-Wahaibi, E.M. El-Sheref, M.M. Hammouda, B.G.M. Youssif, One-pot synthesis of 1-Thia-4-azaspiro[4.4/5]alkan-3-ones via schiff base: design, synthesis, and apoptotic antiproliferative properties of dual EGFR/BRAFV600E inhibitors, Pharmaceuticals 16 (2023) 467–483, https://doi.org/10.3390/ph16030467.
[25] S. Kim, S. Kang, G. Kim, Y. Lee, Copper-catalyzed aza-michael addition of aromatic amines or aromatic aza-heterocycles to α,β-unsaturated olefins, J. Org. Chem. 81 (2016) 4048–4057, https://doi.org/10.1021/acs.joc.6b00341.
[26] A.Y. Rulev, Aza-michael reaction: a decade later – is the research over? Eur. J. Org. Chem. 26 (2023) e202300451 https://doi.org/10.1002/ejoc.202300451.

[27] A. Lozynskyi, B. Zimenkovsky, R. Lesyk, Synthesis and anti-cancer activity of new thiopyrano[2,3-d]thiazoles based on cinnamic acid amides, Sci. Pharm. 82 (2014) 723–734, https://doi.org/10.3797/scipharm.1408-05.
[28] S. Hu-Lieskovan, S. Mok, B.H. Moreno, J. Tsoi, L. Robert, L. Goedert, E. Pinheiro, R. Koya, T. Graeber, B. Comin-Anduix, A. Ribas, Improved antitumor activity of immunotherapy with BRAF and MEK inhibitors in BRAFV600E melanoma, Sci. Transl. Med. 7 (2015), https://doi.org/10.1126/scitranslmed.aaa4691, 279ra41.
[29] M.S. Abdel-Maksoud, M.-R. Kim, M.I. El-Gamal, M.M. Gamal El-Din, J. Tae, H.S. Choi, K.-T. Lee, K.H. Yoo, C.-H. Oh, Design, synthesis, in vitro antiproliferative evaluation, and kinase inhibitory effects of a new series of imidazo[2,1-b]thiazole derivatives, Eur. J. Med. Chem. 95 (2015) 453–463, https://doi.org/10.1016/j.ejmech.2015.03.065.
[30] M.A.I. Elbastawesy, A.A. Aly, Y.A.M.M. El-Shaier, A.B. Brown, G.E.A. Abuo-Rahma, M. Ramadan, New 4-thiazolidinone/quinoline-2-ones scaffold: design, synthesis, docking studies and biological evaluation as potential urease inhibitors, J. Mol. Struct. 1244 (2021) 130845–130855, https://doi.org/10.1016/j.molstruc.2021.130845.
[31] G.M. Sheldrick, SHELXT-integrated space-group and crystal-structure determination, Acta Crystallogr. A71 (2015) 3–8, https://doi.org/10.1107/S2053273314026370.
[32] G.M. Sheldrick, Crystal structure refinement with SHELXL, Acta Crystallogr. C71 (2015) 3–8, https://doi.org/10.1107/S2053229614024218.
[33] A. Saeed, S. Ashraf, U. Flörke, Z.Y.D. Espinoza, M.F. Erben, H. Pérez, Supramolecular self-assembly of a coumarine-based acylthiourea synthon directed by π-stacking interactions: crystal structure and Hirshfeld surface analysis, J. Mol. Struct. 1111 (2016) 76–83, https://doi.org/10.1016/j.molstruc.2016.01.074.
[34] W. Guerrab, I.-M. Chung, S. Kansiz, J. T Mague, N. Dege, J. Taoufik, R. Salghi, I.H. Ali, M.I. Khan, H. Lgaz, Y. Ramli, Synthesis, structural and molecular characterization of 2,2-diphenyl-2H,3H,5H,6H,7H-imidazo[2,1-b][1,3]thiazin-3-one, J. Mol. Struct. 1197 (2019) 369–376, https://doi.org/10.1016/j.molstruc.2019.07.081.
[35] S.D. Kanmazalp, M M, N. Dege, Hirshfeld surface, crystal structure and spectroscopic characterization of (E)-4-(diethylamino)-2-((4-phenoxyphenylimino) methyl) phenol with DFT studies, J. Mol. Struct. 1179 (2019) 181–191, https://doi.org/10.1016/j.molstruc.2018.11.001.